ASEAN Journal for Science and Engineering in Materials

Journal homepage: https://ejournal.bumipublikasinusantara.id/index.php/ajsem

Impact of Relative Humidity on Electrochemical Performance of MXene-Zn-CNC Composite Films

Rudy Fernandez, Hairul Abral[*]*, Ikhwana Elfitri*

Universitas Andalas, Padang, Indonesia
[*]Correspondence: E-mail: abral@eng.unand.ac.id

ABSTRACT

This study examines the influence of relative humidity (RH) on the electrochemical and structural properties of polyvinyl alcohol (PVA) composite films reinforced with MXene, zinc oxide (ZnO), and cellulose nanocrystals (CNC). Composite films were fabricated via solvent casting and conditioned at RH levels of 50%, 75%, and 94%. Cyclic voltammetry and four-point probe tests revealed substantial enhancements in current density, specific capacitance, and bulk conductivity with increasing RH, attributed to improved ionic mobility and interfacial polarization. X-ray diffraction indicated reduced crystallinity due to polymer swelling, while scanning electron microscopy showed enhanced MXene dispersion at higher RH. Fourier-transform infrared spectroscopy confirmed intensified hydroxyl interactions, reflecting increased hydrophilicity. These humidity-induced improvements suggest promising applications in humidity-responsive flexible electronics and sensors. However, potential trade-offs include reduced mechanical stability under prolonged exposure. The findings offer new insights for optimizing hydrophilic polymer composites to enhance environmental adaptability and advanced device performance.

ARTICLE INFO

Article History:
Submitted/Received 08 May 2025
First Revised 09 Jun 2025
Accepted 10 Aug 2025
First Available online 11 Aug 2025
Publication Date 01 Sep 2025

Keyword:
Electrochemical performance,
Humidity-responsive materials,
Ionic conductivity,
MXene,
Polyvinyl alcohol composites.

1. INTRODUCTION

The rapid advancement and proliferation of electronic technologies have significantly amplified electronic waste (e-waste), posing severe environmental and public health challenges globally. E-waste typically comprises complex combinations of hazardous substances, such as heavy metals, flame retardants, and other toxic additives, which, if not managed correctly, result in extensive environmental pollution that affects soil, water, and air quality (Xue *et al*., 2024; Wang *et al*., 2021). The intricate composition of e-waste complicates recycling efforts, leading to inefficient waste management practices that exacerbate ecological degradation. Consequently, there is an urgent need for sustainable and eco-friendly alternatives that not only alleviate environmental harm but also foster responsible resource utilization (Ratwani *et al*., 2024). Recent literature underscores the importance of biodegradable materials as viable solutions, offering significant potential to replace conventional, non-degradable electronic components. Such biodegradable alternatives promise reduced environmental impact due to their enhanced degradability post-consumption, thereby reducing the burden on landfills and minimizing resource depletion.

One promising approach to developing environmentally friendly electronic components involves polymer-based composites utilizing polyvinyl alcohol (PVA) as the matrix material. PVA has garnered considerable attention due to its biodegradability, hydrophilicity, and capacity to integrate various functional fillers, enhancing both its electrical and mechanical properties. Recent studies have demonstrated substantial improvements in electrical performance when fillers such as zinc oxide (ZnO), MXene, and cellulose nanocrystals (CNCs) are incorporated into PVA matrices. Specifically, MXenes, owing to their two-dimensional structures, significantly boost electrical conductivity and facilitate efficient charge transport within composites (Yan *et al*., 2024). Similarly, ZnO has been recognized for enhancing electronic stability, electron mobility, and UV stability due to its semiconductor properties (Wang *et al*., 2022). CNCs reinforce mechanical properties without compromising the composite's inherent flexibility (Li et al., 2022). The synergistic integration of these fillers provides a sustainable and high-performing material solution, aligning perfectly with contemporary objectives in e-waste management and flexible electronic device development.

Fabrication techniques play a critical role in determining the properties and applicability of PVA composite films. One effective method is vacuum-assisted filtration, facilitating uniform dispersion of MXene nanosheets within the PVA matrix, enhancing mechanical and electrical properties, and ensuring a compact microstructure ideal for high conductivity and flexibility (Hu & Li, 2024; Tao *et al*., 2024). Alternatively, solvent casting allows precise control over composition and thickness, significantly influencing the resultant films' electromagnetic interference shielding and mechanical properties, and is widely recognized in polymer composite fabrication (Cui *et al*., 2024). Electrospinning, another prominent method, creates nanofiber structures from PVA/MXene/ZnO solutions, increasing surface area and enhancing intermolecular interactions among components, thus further amplifying the material's functional attributes (Li *et al*., 2022). The integration of these fabrication techniques ensures the development of advanced PVA-based composite films suitable for various electronic applications.

Despite the notable advancements in biodegradable composites, significant challenges remain, particularly concerning the influence of environmental conditions such as relative humidity (RH) on their performance. Humidity substantially impacts the electrical characteristics of hydrophilic polymers, including PVA-based composites, due to their moisture-sensitive nature. Increased moisture absorption at elevated RH levels enhances ionic mobility, creating conductive

pathways that improve electrical conductivity. However, such moisture-induced changes often lead to a trade-off between enhanced electrical performance and compromised mechanical stability and long-term reliability (Li *et al*., 2022). This dichotomy between performance and stability necessitates comprehensive investigations to understand the mechanisms governing humidity-induced electrical changes fully. Previous studies have typically addressed either electrical conductivity or electrochemical capacitance separately, failing to provide a unified understanding of how varying humidity conditions concurrently affect multiple electrical parameters within the same composite system.

Addressing this critical knowledge gap requires an integrated methodological approach, analyzes multiple electrical characteristics simultaneously under controlled humidity conditions. Such an approach promises a holistic understanding of the complex interplay between moisture content and electrical performance. Particularly, there is a distinct lack of studies exploring the comprehensive correlation between current density, specific capacitance derived from cyclic voltammetry (CV), and electrical conductivity measured via the four-point probe method within a single composite system under precisely controlled RH levels. The absence of such integrative analyses limits the potential for developing reliable, humidity-resistant flexible electronic materials and devices suitable for practical applications where environmental conditions vary significantly.

Literature suggests that integrating specific fillers such as MXene, ZnO, and CNC into PVA matrices can offer targeted improvements in electrical performance under humid conditions. For instance, MXene materials have demonstrated exceptional conductivity and flexibility, making them ideal candidates for flexible electronic devices, including strain sensors and electromagnetic interference shielding components (Manibalan & Chen, 2024; Cao et al., 2024). MXenes maintain electrical performance under adverse environmental conditions, particularly high humidity, which is vital for ensuring the reliability of flexible electronic devices (Zheng *et al*., 2025; Cao *et al*., 2024). Meanwhile, CNCs serve an essential role by enhancing dispersion uniformity and mechanical strength in MXene-polymer composites. CNCs effectively prevent agglomeration of MXene sheets, thus maintaining optimal structural integrity and improving mechanical flexibility under stress conditions (Zheng *et al*., 2025; Yan *et al*., 2024). The combination of these fillers has been reported to yield composites with markedly improved mechanical properties, electrical conductivity, and thermal stability, further supporting their suitability for advanced flexible electronics and sensors (Jurečič *et al*., 2024; Wan *et al*., 2021).

Despite promising preliminary findings, significant literature gaps persist regarding how precisely humidity levels modulate ionic conduction pathways and interfacial interactions within these composites. Existing research has inadequately explored how elevated moisture levels influence ionic mobility, interfacial polarization, and mechanical robustness simultaneously. Additionally, the specific role humidity plays in affecting interfacial adhesion between MXene fillers and polymer matrices is understudied, despite its critical impact on maintaining consistent electrical properties in practical applications (Bian *et al*., 2023; Cui *et al*., 2023). Moreover, there is limited information concerning the long-term stability and durability of PVA-based MXene composites under fluctuating humidity conditions, raising valid concerns regarding their viability for real-world applications (Li *et al*., 2022). This scarcity of comprehensive data underscores an urgent need for systematic investigations addressing these specific knowledge gaps.

Here, this study aims to systematically investigate the effect of controlled relative humidity (RH) on the electrochemical and structural performance of biodegradable polyvinyl alcohol (PVA) composite films reinforced with MXene, zinc oxide (ZnO), and cellulose nanocrystals (CNC). The composite films were fabricated via solvent casting and characterized under three RH conditions

(50%, 75%, and 94%) using cyclic voltammetry, four-point probe conductivity measurements, X-ray diffraction, scanning electron microscopy, and Fourier-transform infrared spectroscopy. Unlike previous studies that focused separately on electrical conductivity or capacitance, this work provides an integrated analysis linking ionic conductivity, specific capacitance, crystallinity, morphology, and chemical structure within a single composite system under varying humidity levels. This comprehensive approach offers novel insights into the moisture-structure-performance relationship of MXene-based biodegradable composites, paving the way for the development of high-performance, humidity-responsive flexible electronics and environmental sensors.

2. METHODS

2.1. Materials

In this study, polyvinyl alcohol (PVA), zinc oxide (ZnO), MAX phase precursor for MXene (Ti_3AlC_2), cellulose nanocrystals (CNC), hydrofluoric acid (HF, 40 wt%), sulfuric acid (H_2SO_4, 1 M), silver/silver chloride (Ag/AgCl) reference electrode, and platinum (Pt) counter electrode were utilized. PVA was selected due to its biodegradable nature, hydrophilicity, and compatibility with various conductive fillers. ZnO nanoparticles were chosen for their inherent semiconductor properties and UV stability (Wang *et al*., 2022). CNCs served as mechanical reinforcing agents, ensuring uniform dispersion and improved mechanical robustness within the composite matrix (Li *et al*., 2022). MAX phase precursor (Ti_3AlC_2) and HF were essential for synthesizing MXene, known for its exceptional conductivity and flexibility in composite applications (Yan *et al*., 2024).

2.2. Mxene Etching Procedure

MXene was synthesized through the selective etching of aluminum from the Ti_3AlC_2 MAX phase using hydrofluoric acid (HF). Specifically, the MAX phase powder was gradually added to the HF solution and stirred continuously for 24 hours at room temperature, ensuring complete aluminum removal. Post-etching, the MXene suspension was washed multiple times with deionized water to neutralize residual HF, as evidenced by reaching a neutral pH level. The washed MXene nanosheets were then separated via centrifugation and dried under vacuum at 60°C for 12 hours, resulting in a fine MXene powder suitable for composite fabrication.

2.3. Film Fabrication

Composite films of PVA/ZnO/MXene/CNC were fabricated using a sequential dispersion and solvent casting method, enabling precise control over film thickness and composition (Cui *et al*., 2024). Initially, PVA was dissolved in deionized water at 80°C under constant magnetic stirring until a clear homogeneous solution was achieved. Subsequently, predetermined quantities of ZnO nanoparticles, MXene nanosheets, and CNC were sequentially dispersed into the PVA solution under continuous ultrasonication for 8 minutes, ensuring homogeneous mixing and minimizing agglomeration. The mixture was further stirred at 80°C to maintain dispersion uniformity before casting onto a glass substrate. The cast films were dried in a vacuum oven at 60°C for 24 hours, ensuring the removal of residual moisture and the formation of uniformly thick composite films. Vacuum-assisted filtration and electrospinning methods are alternative approaches known to enhance uniform dispersion and composite film functionality, contributing significantly to their conductive and mechanical properties (Hu & Li, 2024; Li et al., 2022). **Figure 1** illustrates the workflow employed in the composite film fabrication.

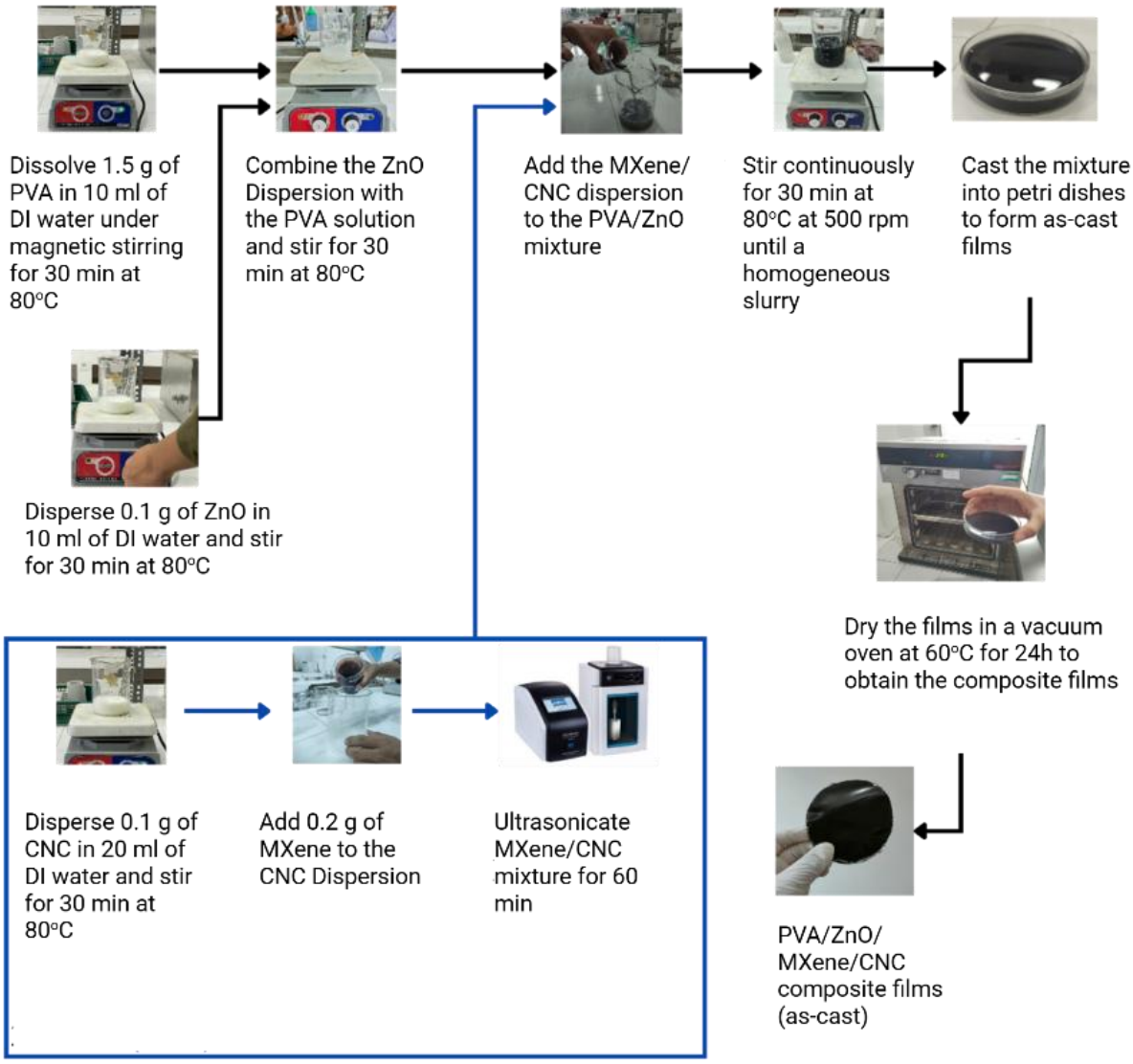

Figure 1. Workflow of PVA/ZnO/MXene/CNC composite film production

2.4. Humidity Conditioning

Prepared composite films underwent humidity conditioning to assess performance changes under different relative humidity (RH) environments. Films were equilibrated for 48 hours within desiccators precisely controlled at three distinct humidity levels: 50, 75, and 94% RH. The humidity conditioning setups enabled controlled, stable moisture environments, crucial for systematically evaluating humidity-induced variations in composite film properties.

2.5. Electrical testing

Electrical characterization included cyclic voltammetry (CV) and four-point probe measurements, standard methods widely recognized for evaluating electrode and film performance under controlled humidity conditions (Zhang *et al*., 2024; Fang *et al*., 2020).

CV tests were performed using an electrochemical workstation with a three-electrode configuration consisting of the composite film as the working electrode, Ag/AgCl as the reference electrode, and Pt as the counter electrode. The electrolyte utilized was 1 M sulfuric acid (H_2SO_4). The voltage sweep range was set between 0 and 0.8 V at a scan rate conducive to accurately

capturing the current density (J) and specific capacitance (C_{sp}) responses influenced by ionic mobility and hydration effects at varying RH levels.

Four-point probe tests assessed the bulk electrical conductivity (σ) of the composite films, eliminating errors from contact resistance commonly encountered in two-point measurements. Four equally spaced probes were placed in direct contact with the films, facilitating accurate resistance measurements. Conductivity values were subsequently calculated by converting measured resistances, thus providing insights into the intrinsic electrical properties of the films as influenced by moisture absorption at different humidity conditions (Liu *et al*., 2023).

2.6. Characterization

Surface morphology, crystallinity, and chemical structure of the composite films were meticulously characterized to correlate structural attributes with electrical performance. Scanning electron microscopy (SEM) analysis was conducted at 5000× magnification, elucidating the surface morphology, particle distribution, and agglomeration patterns, particularly the dispersion and interaction of MXene nanosheets facilitated by CNC fillers. Detailed information regarding the SEM analysis method is explained elsewhere (Yolanda & Nandiyanto, 2022).

X-ray diffraction (XRD) patterns were acquired to evaluate crystallinity changes within the films as a function of humidity exposure. Peak deconvolution analysis enabled precise quantification of crystallinity shifts, thus linking structural order variations directly to conductivity and mechanical properties. Detailed information regarding the XRD analysis method is explained elsewhere (Fatimah *et al*., 2022; Tomaszewski, 2023)

Fourier-transform infrared spectroscopy (FTIR) was employed to analyze chemical group interactions, focusing specifically on hydrophilic shifts and hydrogen bonding dynamics among film components at various RH levels. FTIR spectra offered crucial evidence regarding the nature and extent of chemical changes responsible for the observed improvements in ionic conduction and interfacial polarization. Detailed information regarding the FTIR analysis method is explained elsewhere (Nandiyanto *et al*., 2019; Nandiyanto *et al*., 2023; Sukamto & Rahmat, 2023).

2.7. Data processing and statistical analysis

Data obtained from cyclic voltammetry and conductivity measurements were rigorously analyzed by averaging across four consecutive CV cycles, providing statistically robust results. The changes in electrical parameters were quantified as percentage changes relative to baseline conditions (50% RH), enabling clear visualization of humidity-induced performance trends. Possible sources of experimental error, including equipment calibration, electrode preparation consistency, and measurement reproducibility, were critically assessed to ensure the reliability and accuracy of reported data.

Together, these methodological approaches facilitated a comprehensive understanding of how controlled humidity conditions systematically influenced the performance attributes of PVA/ZnO/MXene/CNC composite films, guiding the development of robust, flexible, and eco-friendly electronic materials.

3. RESULTS AND DISCUSSION

3.1. Characterization

The polyvinyl alcohol (PVA) composite films incorporating MXene, ZnO, and cellulose nanocrystals (CNC) consistently demonstrated robust physical characteristics. The films, fabricated through solvent casting methods, exhibited uniform dimensions, approximately 10 cm in diameter and thicknesses around 0.25 mm, ensuring reproducibility and reliable performance metrics. Their homogeneous and flexible structure, coupled with a distinct black coloration,

indicated effective and uniform dispersion of MXene nanosheets, ZnO particles, and CNC within the polymer matrix. Uniform morphology is pivotal as it enhances electrical stability by creating continuous conductive pathways throughout the composite, crucial for consistent performance (Li *et al*., 2022; Hu & Li, 2024). **Figure 2** depicts this composite film after fabrication.

Figure 2. Photograph image of the as-cast composite film.

3.2. Electrochemical Response (CV)

Electrochemical characterization using cyclic voltammetry (CV) revealed pronounced enhancements in the electrochemical responses of the composite films under varying relative humidity (RH) levels. At lower humidity conditions (50% RH), the films exhibited modest electrochemical activity, presenting a current density (J) of 2.86×10^{-5} A/cm^2. With an increase to 75% RH, the current density sharply rose to 9.09×10^{-5} A/cm^2, an improvement of roughly 217.3%. Further increasing the RH to 94% dramatically boosted current density to 0.408×10^{-5} A/cm^2, signifying an overall remarkable enhancement of approximately 349% from baseline. Correspondingly, the specific capacitance (C_{sp}) significantly increased from 0.106×10^{-5} F/g at 50% RH to 0.629×10^{-5} F/g at 94% RH, a substantial increment of 191.97% (**Table 1**). Voltammogram shapes further supported these findings, becoming increasingly rectangular at higher humidity, clearly indicating capacitive behavior dominated by rapid ionic interactions at the composite's surface. These observations are consistent with previously published literature, confirming that increased humidity significantly facilitates ionic mobility and surface charge availability (Ratwani *et al*., 2024; Lee *et al*., 2023; Xu *et al*., 2022). **Figures 3(a-c)** graphically summarize the detailed CV results, elucidating these notable trends.

Table 1. Current density (J) and Specific capacitance (C_{sp}) at Various RH levels (means ± SD).

Relative Humidity (RH)	Current Density (A/cm^2)	Specific Capacitance (F/g)
50%	2.86×10^{-5}	1.06×10^{-4}
75%	9.09×10^{-5}	2.16×10^{-4}
94%	0.408×10^{-5}	6.29×10^{-4}

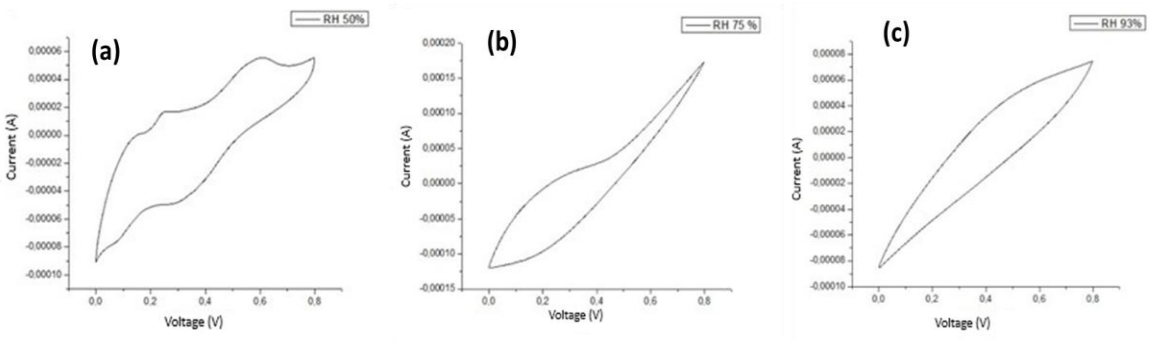

Figure 3. Results: (a) CV for 50% RH; (b) CV for 75% RH; and (c) CV for 94% RH.

3.3. Bulk Conductivity (4-Point Probe)

Bulk electrical conductivity measurements via the four-point probe technique demonstrated a consistent positive correlation with humidity, peaking notably at 94% RH. The conductivity values increased from an initial 0.902 S/cm at 50% RH to a substantial 1.227 S/cm at 94% RH (**Table 2**). Enhanced conductivity at elevated humidity levels results predominantly from intensified water absorption into the composite films, thereby promoting stronger ionic pathways and reinforcing interactions between the hydroxyl groups present in the PVA matrix and the fillers. Such findings align closely with previously documented evidence on hydrophilic polymer composites, which emphasize the essential role of water molecules in facilitating ionic conduction pathways (Lee et al., 2023; Zhang et al., 2024). **Figure 4** effectively illustrates this humidity-dependent trend, underscoring its potential impact on practical applications such as flexible electronics and energy storage devices.

Table 2. Resistance and conductivity values at different RH levels.

Relative Humidity (RH)	Resistance (Ω)	Conductivity (S/cm)	Film Thickness (mm)
50%	11.487	0.902	0.25 ± 0.01
75%	7.5974	1.118	0.25 ± 0.01
94%	5.4506	1.227	0.25 ± 0.01

The integration of cyclic voltammetry (CV) and four-point probe conductivity tests provided a coherent correlation between electrochemical and electrical conductivity performance, affirming the hypothesis that increased RH significantly enhances ionic transport within these composites. Specifically, CV-derived measurements of specific capacitance demonstrated substantial enhancements concurrently with bulk conductivity measurements from the four-point probe method. This coherent correlation supports the role of moisture-driven ion mobility improvements. Enhanced ionic conductivity at elevated humidity conditions has been consistently reported across polymer-based composite systems, reinforcing the notion that environmental moisture plays a central role in modulating electrical performance, as validated in prior studies (Lee et al., 2023; Zhang et al., 2024).

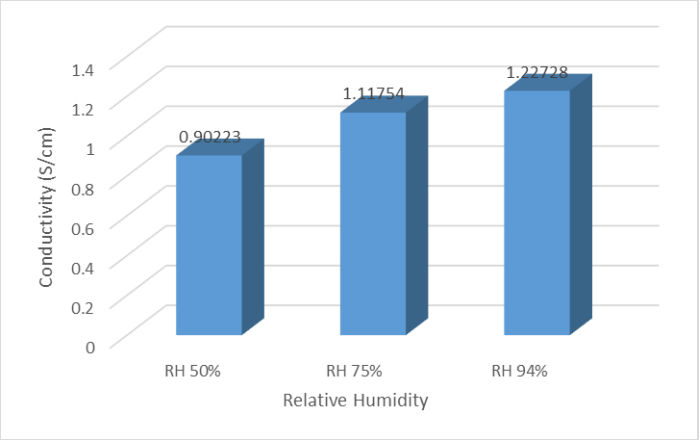

Figure 4. Conductivity values achieved at different RH levels.

3.4. Crystallinity (XRD)

X-ray diffraction (XRD) analyses indicated a clear and significant reduction in crystallinity within the composite films as humidity increased. Crystallinity levels declined from 11.93% at 50% RH to 8.44% at 94% RH. This trend correlates strongly with swelling behaviour induced by increased moisture, disrupting ordered crystalline regions and facilitating ionic mobility crucial for improved electrochemical performance. Similar outcomes are documented in the literature, confirming the association between decreased crystallinity and enhanced ionic conduction (Li *et al*., 2022; Hu & Li, 2024). The XRD patterns shown in **Figures 5 (a-c)** distinctly illustrate these humidity-induced structural transformations, directly linking reduced crystallinity to increased ionic mobility and conductivity.

Such structural transitions from crystalline to amorphous domains facilitate ionic mobility; however, they concurrently compromise mechanical robustness, potentially limiting practical application under conditions of prolonged exposure to elevated humidity (Malik *et al*., 2022). Although these humidity-induced alterations significantly boost electrochemical performance, the long-term stability and cyclic durability under repeated humidity fluctuations remain unaddressed and represent a critical area for future investigation. Understanding the long-term implications of moisture-driven morphological changes on mechanical integrity and electrical stability will be indispensable for the practical deployment of these composite materials.

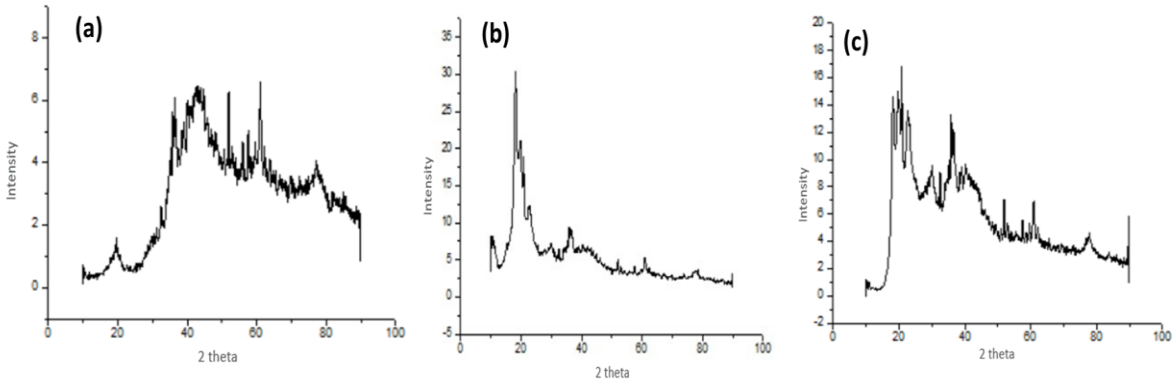

Figure 5. XRD results: (a) 50% RH; (b) 75% RH; and (c) 94% RH.

3.5. Morphology (SEM)

Scanning electron microscopy (SEM) provided detailed visualization of morphological changes in composite films subjected to varying humidity conditions. At lower humidity (50%), films exhibited smooth, uniform surfaces indicative of stable microstructures. In contrast, elevated humidity conditions led to pronounced surface agglomerations caused by polymer swelling and moisture absorption. Interestingly, despite these morphological changes, the higher humidity significantly improved MXene dispersion within the polymer matrix. Enhanced hydrogen bonding facilitated by absorbed water molecules likely contributed to improved nanosheet distribution, subsequently enhancing conductive pathways and electrochemical performance (Bian *et al*., 2023; Hassan *et al*., 2024). **Figure 6 (a-c)** provides representative SEM micrographs demonstrating these morphological shifts and their implications for electrical performance enhancements.

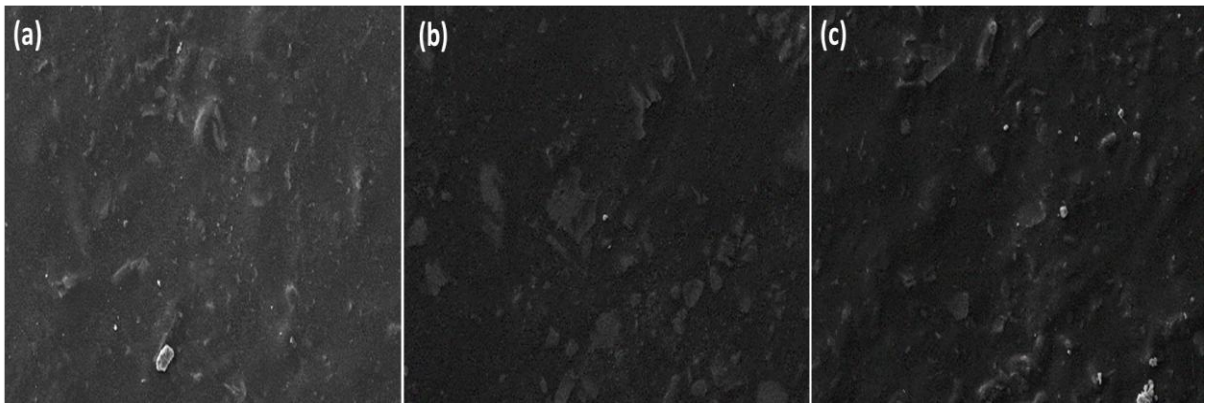

Figure 6. SEM micrograph images (5000x): (a) 50% RH; (b) 75% RH; and (c) 94% RH.

Fourier-transform infrared spectroscopy (FTIR) analysis demonstrated significant chemical structural changes within composite films at elevated humidity levels, primarily indicated by intensified hydroxyl (–OH) stretching bands. These spectral changes reflect increased hydrophilicity and more pronounced hydrogen bonding due to moisture uptake, which significantly facilitates ionic mobility and electrical conductivity improvements. Such observations align with previous research emphasizing the crucial role of enhanced hydrogen bonding interactions in augmenting the electrochemical properties of polymer composites under humid conditions (Zhang *et al*., 2024; Yu *et al*., 2022). **Figures 7(a-b)** provide visual confirmation of these humidity-induced chemical structural modifications.

The comprehensive investigation confirms that humidity-induced enhancements in ionic conductivity and electrochemical performance primarily result from increased moisture uptake, facilitating enhanced ionic mobility and interfacial polarization within the composite structure. Each filler within the composite contributes uniquely to its performance: MXene nanosheets function as primary conductive pathways, CNC fillers mitigate MXene agglomeration and improve mechanical stability, and ZnO particles offer enhanced semiconductor characteristics and mechanical robustness (Wang *et al*., 2022; Cui *et al*., 2023).

However, these humidity-driven improvements introduce notable trade-offs, particularly polymer swelling and decreased crystallinity, potentially reducing mechanical durability and structural integrity during extended exposure to elevated humidity. Addressing these limitations is crucial for the future practical application of these composites, emphasizing the need for additional research into long-term stability under cyclic humidity conditions (Malik *et al*., 2022).

Comparative analysis with existing literature reinforces the promising nature of these findings, validating their application potential in humidity-sensitive sensors and flexible electronic devices.

Effective humidity management strategies, including encapsulation and environmental control, become vital considerations for practical device design (Ren *et al*., 2024; Su *et al*., 2022).

Collectively, this detailed examination highlights the critical interplay between humidity conditions, structural transformations, and electrochemical performance. The insights presented significantly contribute to advancing the development of robust, humidity-responsive polymer composites suitable for diverse applications in flexible electronics, environmental sensors, and energy storage technologies.

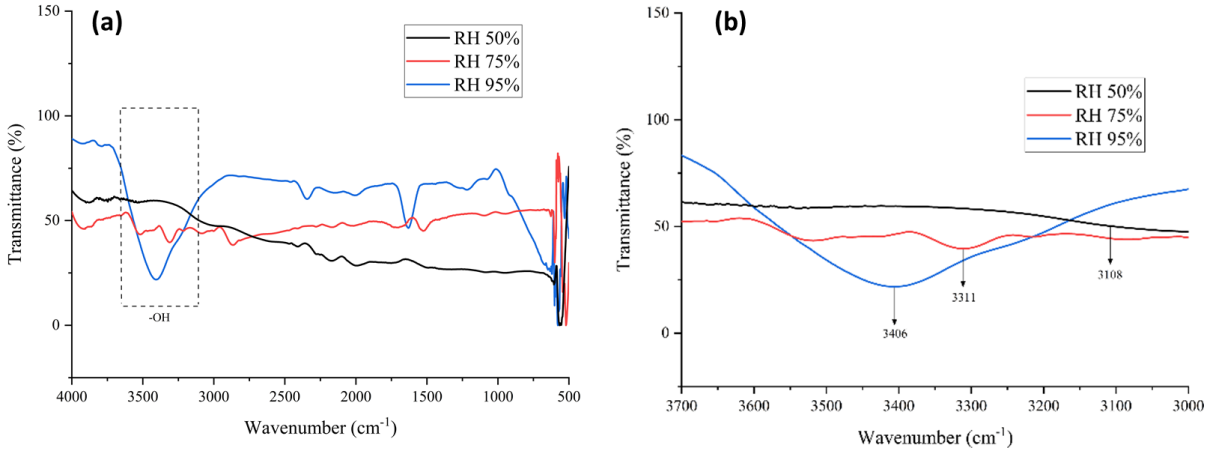

Figure 7. FTIR results: (a) FTIR Spectra of OH groups at different RH levels, and (b) enlarged view of the dashed line region.

4. CONCLUSION

This study systematically investigated the influence of relative humidity (RH) on the electrochemical and structural properties of polyvinyl alcohol (PVA)-based composite films reinforced with MXene, zinc oxide (ZnO), and cellulose nanocrystals (CNC). Results confirmed that higher RH significantly enhances ionic conductivity, specific capacitance, and bulk conductivity, attributed primarily to increased water adsorption facilitating enhanced ionic mobility and interfacial polarization at the PVA–water–MXene interfaces. Concurrently, humidity-induced structural transitions towards a more amorphous state markedly decreased crystallinity, positively impacting ionic transport yet potentially compromising long-term mechanical stability. Morphological analysis revealed improved dispersion of MXene nanosheets at elevated humidity, essential for optimized conductive pathways. Chemically, intensified hydroxyl bonding interactions at high RH were identified, correlating strongly with increased ionic mobility and electrochemical performance. These findings expand current knowledge on the interplay between environmental conditions and the functional performance of hydrophilic polymer composites, offering vital insights for designing advanced humidity-responsive flexible electronics and sensors. Future research should address long-term mechanical stability, cyclic humidity exposure impacts, and practical encapsulation strategies to harness the full potential of these composites.

5. ACKNOWLEDGMENT

We gratefully acknowledge the Laboratorium Penelitian – Departemen Teknik Lingkungan and the Laboratorium Material Teknik – Departemen Teknik Mesin, Universitas Andalas, for facilitating the testing and measurements for this research.

6. AUTHORS' NOTE

The authors declare that there is no conflict of interest regarding the publication of this article. The authors confirmed that the paper was free of plagiarism

7. REFERENCES

Bian, X., Yang, Z., Zhang, T., Yu, J., Xu, G., Chen, A., He, Q., and Pan, J. (2023). Multifunctional flexible AgNW/MXene/PDMS composite films for efficient electromagnetic interference shielding and strain sensing. *ACS Applied Materials and Interfaces*, *15*(35), 41906–41915.

Cao, J., Jiang, Y., Li, X., Yuan, X., Zhang, J., He, Q., Ye, F., Geng, L., Guo, S., Zhang, Y., and Wang, Q. (2024). A flexible and stretchable MXene/Waterborne polyurethane composite-coated fiber strain sensor for wearable motion and healthcare monitoring. *Sensors*, *24*(1), 271.

Cui, X., Miao, C., Lu, S., Liu, X., Yang, Y., and Jingchao, S. (2023). Strain sensors made of MXene, CNTs, and TPU/PSF asymmetric structure films with large tensile recovery and applied in human health monitoring. *ACS Applied Materials and Interfaces*, *15*(51), 59655–59670.

Cui, Y., Ru, G., Zhang, T., Yang, K., Liu, S., Qi, W., Ye, Q., Liu, X., and Zhou, F. (2024). Schottky Interface Engineering in Ti_3C_2Tx/ZnS organic hydrogels for high-performance multifunctional flexible absorbers. *Advanced Functional Materials*, *35*(11).

Fang, Y., Lian, R., Li, H., Zhang, Y., Gong, Z., Zhu, K., Ye, K., Yan, J., Wang, G., Gao, Y., Wei, Y., and Cao, D. (2020). Induction of planar sodium growth on MXene (Ti_3C_2Tx)-modified carbon cloth hosts for flexible sodium metal anodes. *ACS Nano*, *14*(7), 8744–8753.

Fatimah, S., Ragadhita, R., Al Husaeni, D.F., and Nandiyanto, A.B.D. (2022). How to calculate crystallite size from X-ray diffraction (XRD) using Scherrer method. *ASEAN Journal of Science and Engineering*, *2*(1), 65-76.

Guo, M., Yuan, C., Xu, T., Zhong, S., Wang, W., Zou, T., Zhang, T., and Yu, X. (2023). In situ built nanoconfined TiO_2 particles in robust-flexible MXene@rGO conductive framework enabling high-performance hybrid magnesium–sulfur batteries. *Advanced Energy Materials*, *13*(26), 2300417.

Hassan, M., Li, P., Lin, J., Li, Z., Javed, M. S., Peng, Z., and Çelebi, K. (2024). Smart energy storage: W18O49 NW/Ti_3C_2Tx composite-enabled all solid state flexible electrochromic supercapacitors. *Small*, *20*(33), 2400278.

Hu, S., and Li, S. (2024). Flexible and conductive polyvinyl alcohol/Ti3C2Tx composite film with excellent electromagnetic interference shielding performance. *International Conference on Computer Technology, Information Engineering, and Electron,* 12987, 180-185.

Huang, Y., and Bian, S. (2024). Free-Standing MXene/Carbon Nanotube@Fe2O3 Film Electrodes With High Capacitance for All-in-One Supercapacitors. *ACS Applied Energy Materials*, *7*(22), 10358–10366.

Jurečič, V., Lakshmanan, S., Novak, N., Kokol, V., and Bobnar, V. (2024). Percolative dielectric behavior of titanium carbide MXene/cellulose nanofibrils composite films. *APLl Materials*, *12*(11), 111102.

Kim, S., Kang, C., Choi, T., Kim, J., and Kim, H. (2023). Conformal passivation of self-cleanable, flexible, and transparent polytetrafluoroethylene thin films on two-dimensional MXene and

three-dimensional Ag nanowire composite electrodes. *ACS Applied Electronic Materials*, *5*(3), 1636–1649.

Lee, S., Nguyen, N. K., Kim, W., Kim, M., Cao, V., and Nah, J. (2023). Absorption-dominant electromagnetic interference shielding through electrical polarization and triboelectrification in surface-patterned ferroelectric poly[(vinylidenefluoride-co-trifluoroethylene)-MXene] composite. *Advanced Functional Materials*, *33*(43), 2307588.

Li, H., Ru, X., Song, Y., Wang, H., Yang, C., Zheng, S., Gong, L., Zhang, X., Duan, H., Liu, Z., Zhang, Q., and Chen, Y. (2022). Flexible sandwich-structured silicone rubber/MXene/Fe_3O_4 composites for tunable electromagnetic interference shielding. *Industrial amd Engineering Chemistry Research*, *61*(32), 11766–11776.

Li, J., Li, Y., Yang, L., and Yin, S. (2022). Ti_3C_2Tx/pani/liquid metal composite microspheres with 3D nanoflower structure: Preparation, characterization, and applications in EMI shielding. *Advanced Materials Interfaces*, *9*(10), 2102266.

Li, L., Ji, X., and Chen, K. (2022). Conductive, self-healing, and antibacterial Ag/MXene-PVA hydrogel as wearable skin-like sensors. *Journal of Biomaterials Applications*, *37*(7), 1169–1181.

Liu, H., Chen, X., Zheng, Y., Zhang, D., Zhao, Y., Wang, C., Pan, C., Liu, C., and Shen, C. (2021). Lightweight, superelastic, and hydrophobic polyimide nanofiber /MXene composite aerogel for wearable piezoresistive sensor and oil/water separation applications. *Advanced Functional Materials*, *31*(13), 2008006.

Liu, Z., Zhang, Y., Song, Y., Lu, Y., Liu, T., and Zhang, J.-C. (2023). A wearable 3D pressure sensor based on electrostatic self-assembly MXene/chitosan sponge and insulating PVP spacer. *Nanotechnology*, *34*(45), 455502.

Luan, H., Zhang, D., Xu, Z., Zhao, W., Yang, C., and Chen, X. (2022). MXene-based composite double-network multifunctional hydrogels as highly sensitive strain sensors. *Journal of Materials Chemistry C*, *10*(19), 7604–7613.

Malik, R., Parida, R., Parida, B. N., and Nayak, N. C. (2022). Structural, thermal and dielectric properties of 2D layered Ti_3C_2Tx (MXene) filled poly (Ethylene-co-methyl Acrylate) (EMA) nanocomposites. *Journal of Applied Polymer Science*, *140*(6), e53460.

Manibalan, K., and Chen, J. (2024). Recent progress on MXene–polymer composites for soft electronics applications in sensing and biosensing: A review. *Journal of Materials Chemistry A*, *12*(40), 27130–27156.

Nandiyanto, A.B.D., Oktiani, R., and Ragadhita, R. (2019). How to read and interpret FTIR spectroscope of organic material. *Indonesian Journal of Science and Technology*, *4*(1), 97-118.

Nandiyanto, A.B.D., Ragadhita, R., and Fiandini, M. (2023). Interpretation of Fourier Transform Infrared Spectra (FTIR): A practical approach in the polymer/plastic thermal decomposition. *Indonesian Journal of Science and Technology*, *8*(1), 113-126.

Obinna, E.N. (2022). Physicochemical properties of human hair using Fourier Transform Infra-Red (FTIR) and Scanning Electron Microscope (SEM). *ASEAN Journal for Science and Engineering in Materials*, *1*(2), 71-74.

Qin, L., Tao, Q., Ghazaly, A. E., Fernández-Rodríguez, J., Persson, P. O. Å., Rosén, J., and Zhang, F. (2017). High-performance ultrathin flexible solid-state Supercapacitors based on solution processable Mo1.33C MXene and PEDOT: PSS. *Advanced Functional Materials*, *28*(2), 1703808.

Ratwani, C. R., Demko, D., Bakhit, B., Kamali, A. R., and Abdelkader, A. M. (2024). Tuning surface terminations and hydration interactions in MXene nanosheet-based hydrogel composites for self-healable strain sensors. *ACS Applied Nano Materials*, *7*(17), 20196–20205.

Ren, J., Huang, X., Han, R., Chen, G., Zhou, Z., and Li, Q. (2023). An extreme condition-resistant superelastic silica nanofiber/MXene composite aerogel for synchronous sensing and thermal management. *Journal of Materials Chemistry A*, *11*(19), 10396–10412.

Ren, S., Pan, X., Zhang, Y., Xu, J., Liu, Z., Zhang, X., Li, X., Gao, X., Zhong, Y., Chen, S., and Wang, S. (2024). Conductive MXene/polymer composites for transparent flexible supercapacitors. *Small*, *20*(35), 2401346.

Ren, Z., Guo, F., Wen, Y., Yang, Y., Liu, J., and Cheng, S. (2024). Strong and anti-swelling nanofibrous hydrogel composites inspired by biological tissue for amphibious motion sensors. *Materials Horizons*, *11*(22), 5600–5613.

Su, Y., Ma, K., Mao, X., Liu, M., and Zhang, X. (2022). Highly Compressible and sensitive flexible piezoresistive pressure sensor based on MWCNTs/Ti3C2Tx MXene @ melamine foam for human gesture monitoring and recognition. *Nanomaterials*, *12*(13), 2225.

Sukamto, S., and Rahmat, A. (2023). Evaluation of FTIR, macro and micronutrients of compost from black soldier fly residual: In context of its use as fertilizer. *ASEAN Journal of Science and Engineering*, *3*(1), 21-30.

Tao, D., Yang, C., Chen, C., Kun, Y., You, H., Wang, W., and Wang, D. (2024). Highly flexible and ultralight PVA-co-PE-AgNW/MXene composite film with low filling for multistage electromagnetic interference shielding. *Small*, *21*(7), 2411752.

Tomaszewski, P. E. (2023). Comments on the paper “How to calculate crystallite size from x-ray diffraction (XRD) using Scherrer method” by Siti Fatimah et al. published in ASEAN Journal of Science and Engineering 2 (2022) 65. *ASEAN Journal of Science and Engineering*, *3*(3), 301-304.

Wan, Y., Xiong, P., Liu, J., Feng, F., Xun, X., Gama, M., Zhang, Q., Yao, F., Yang, Z., Luo, H., and Xu, Y. (2021). Ultrathin, strong, and highly flexible Ti_3C_2Tx MXene/bacterial cellulose composite films for high-performance electromagnetic interference shielding. *ACS Nano*, *15*(5), 8439–8449.

Wang, G., Yang, Z., Li, L., Ren, J., Liu, J., and Li, L. (2024). Self-assembled MXene@Fluorographene hybrid for high dielectric constant and low loss ferroelectric polymer composite films. *ACS Applied Materials and Interfaces*, *16*(19), 25268–25279.

Wang, J., Ma, X., Zhou, J., Du, F., and Teng, C. (2022). Bioinspired, high-strength, and flexible mxene/aramid fiber for electromagnetic interference shielding papers with joule heating performance. *ACS Nano*, *16*(4), 6700–6711.

Wang, P., Jian, M., Zhang, C., Wu, M., Ling, X., Zhang, J., Wei, B., and Yang, L. (2021). Highly stable graphene-based flexible hybrid transparent conductive electrodes for organic solar cells. *Advanced Materials Interfaces*, *9*(3), 2101442.

Weng, G., Li, J., Alhabeb, M., Karpovich, C., Wang, H., Lipton, J., Maleski, K., Kong, J., Shaulsky, E., Elimelech, M., Gogotsi, Y., and Taylor, A. D. (2018). Layer-by-layer assembly of cross-functional semi-transparent MXene-carbon nanotubes composite films for next-generation electromagnetic interference shielding. *Advanced Functional Materials*, *28*(44), 1803360.

Xu, H., Chen, G., Du, F., Wang, X., Dall'Agnese, Y., and Gao, Y. (2022). Electrospun Ti_3C_2Tx MXene and silicon embedded in carbon nanofibers for lithium-ion batteries. *Journal of Physics D Applied Physics*, *55*(20), 204002.

Xue, H., Huang, P., Göthelid, M., Strömberg, A., Niklaus, F., and Li, J. (2024). Ultrahigh-rate on-paper PEDOT:PSS-Ti_2C microsupercapacitors with large areal capacitance. *Advanced Functional Materials*, *34*(49), 2409210.

Yan, S., Zhang, H., Li, L., Fu, Q., and Ge, X. (2024). Flexible and recyclable MXene nanosheet/Ag nanowire/cellulose nanocrystal composite films for electromagnetic interference shielding. *ACS Applied Nano Materials*, *7*(3), 2702–2710.

Yolanda, Y.D., and Nandiyanto, A.B.D. (2022). How to read and calculate diameter size from electron microscopy images. *ASEAN Journal of Science and Engineering Education, 2*(1)*,* 11-36.

Yu, Q., Su, C., Bi, S., Huang, Y., Li, J., Shao, H., Jiang, J., and Chen, N. (2022). Ti3C2Tx@nonwoven fabric composite: Promising MXene-coated fabric for wearable piezoresistive pressure sensors. *ACS Applied Materials and Interfaces*, *14*(7), 9632–9643.

Zhan, Z., Song, Q., Zhou, Z., and Lu, C. (2019). Ultrastrong and conductive MXene/cellulose nanofiber films enhanced by hierarchical nano-architecture and interfacial interaction for flexible electromagnetic interference shielding. *Journal of Materials Chemistry C*, *7*(32), 9820–9829.

Zhang, K., Sun, J., Song, J., Gao, C., Wang, Z., Song, C., Wu, Y., and Liu, Y. (2020). Self-healing Ti3C2 MXene/PDMS supramolecular elastomers based on small biomolecules modification for wearable sensors. *ACS Applied Materials and Interfaces*, *12*(40), 45306–45314.

Zhang, P., Li, Y., Zhang, H., Li, Y., Yin, X., Zheng, W., Ding, J., and Sun, Z. (2024). Microporous tungsten oxide spheres coupled with Ti_3C_2Tx nanosheets for high-volumetric capacitance supercapacitors. *Nanotechnology*, *35*(49), 495401.

Zhang, P., Sui, Y., Ma, W., Duan, N., Liu, Q., Zhang, B., Niu, H., and Qin, C. (2023). Tightly intercalated Ti_3C_2Tx/MoO_3–x/Pedot:PSS Free-standing films with high volumetric/gravimetric performance for flexible solid-state supercapacitors. *Dalton Transactions*, *52*(3), 710–720.

Zhang, S., Ying, H., Huang, P., Wang, J., Zhang, Z., Zhang, Z., and Han, W. (2021). Ultrafine Sb pillared few-layered Ti_3C_2Tx MXenes for advanced sodium storage. *ACS Applied Energy Materials*, *4*(9), 9806–9815.

Zhang, X., Sun, H., Zhang, J., and Wang, Z. (2024). A Highly sensitive and stable mxene/bacterial cellulose double network hydrogel flexible strain sensor for human activities monitoring. *Journal of Applied Polymer Science*, *142*(6), e56468.

Zhang, Y., Chang, T., Jing, L., Li, K., Yang, H., and Chen, P. (2020). Heterogeneous, 3D architecturing of 2D titanium carbide (MXene) for microdroplet manipulation and voice recognition. *ACS Applied Materials and Interfaces*, *12*(7), 8392–8402.

Zheng, Z., Song, S., Chen, X., Li, X., and Li, J. (2025). Ultra-stretchable polymer fibers anchored with a triple-level self-assembled conductive network for wide-range strain detection. *Polymers*, *17*(6), 734.

Zhou, J., Yu, J., Shi, L., Wang, Z., Liu, H., Yang, B., Li, C., Zhu, C., and Xu, J. (2018). A conductive and highly deformable all-pseudocapacitive composite paper as supercapacitor electrode with improved areal and volumetric capacitance. *Small*, *14*(51), 1803786.